LETTER

doi:10.1038/nature12759

# Stabilizing the magnetic moment of single holmium atoms by symmetry

Toshio Miyamachi[1,2], Tobias Schuh[1], Tobias Märkl[1], Christopher Bresch[1], Timofey Balashov[1], Alexander Stöhr[1,3], Christian Karlewski[4], Stephan André[4], Michael Marthaler[4], Martin Hoffmann[5,6], Matthias Geilhufe[5], Sergey Ostanin[5], Wolfram Hergert[6], Ingrid Mertig[5,6], Gerd Schön[4], Arthur Ernst[5,7] & Wulf Wulfhekel[1]

**Single magnetic atoms, and assemblies of such atoms, on non-magnetic surfaces have recently attracted attention owing to their potential use in high-density magnetic data storage and as a platform for quantum computing[1–8]. A fundamental problem resulting from their quantum mechanical nature is that the localized magnetic moments of these atoms are easily destabilized by interactions with electrons, nuclear spins and lattice vibrations of the substrate[3–5]. Even when large magnetic fields are applied to stabilize the magnetic moment, the observed lifetimes remain rather short[5,6] (less than a microsecond). Several routes for stabilizing the magnetic moment against fluctuations have been suggested, such as using thin insulating layers between the magnetic atom and the substrate to suppress the interactions with the substrate's conduction electrons[2,3,5], or coupling several magnetic moments together to reduce their quantum mechanical fluctuations[7,8]. Here we show that the magnetic moments of single holmium atoms on a highly conductive metallic substrate can reach lifetimes of the order of minutes. The necessary decoupling from the thermal bath of electrons, nuclear spins and lattice vibrations is achieved by a remarkable combination of several symmetries intrinsic to the system: time reversal symmetry, the internal symmetries of the total angular momentum and the point symmetry of the local environment of the magnetic atom.**

In a free atom the net spin and orbital angular momenta couple to the total angular momentum $\boldsymbol{J}$, resulting in an atomic magnetic moment. The continuous rotation symmetry means that the $2J+1$ magnetic sub-levels $J_z = -J,\ -J+1,\ \ldots\ +J$ are degenerate in the absence of a magnetic field $\boldsymbol{B}$, as illustrated in Fig. 1a. If the atom is prepared in a specific magnetic state, this state is not stable against the slightest interaction of $\boldsymbol{J}$ with the environment, for example, with a thermal bath of electrons or nuclear spins, leading—without an energy cost—to transitions to other magnetic states and, hence, to a loss of orientation of the magnetic moment. Even the measurement of the magnetic state represents such an interaction.

The magnetic moment of an atom in a memory cell or quantum device can be stabilized by placing the atom on a substrate where the electrostatic interaction with the neighbouring atoms gives rise to magnetic anisotropy. This crystal field splits the formerly degenerate magnetic states. A decade ago, a giant magnetic anisotropy was discovered for single Co atoms on the Pt(111) surface[1]. Because of the broken inversion symmetry, a magnetic moment oriented normal to the surface plane is preferred over an in-plane orientation (the normal orientation is 9.3 meV lower in energy). To lowest order, this uniaxial anisotropy can be described by a simple crystal-field Hamiltonian $\mathcal{H} = D J_z^2$, where $D$ is the uniaxial anisotropy constant. Figure 1b depicts the resulting states in a shape of a down-turned parabola ($D<0$) with the two degenerate ground states $|+J\rangle$ and $|-J\rangle$.

The main mechanism for magnetization reversal are spin-flip events mediated by the exchange interaction with substrate electrons. The interaction operator can be written as:

$$\mathcal{V} = \boldsymbol{J}\cdot\boldsymbol{\sigma} = J_z\sigma_z + \frac{1}{2}\left(J_+\sigma_- + J_-\sigma_+\right), \qquad (1)$$

where $\boldsymbol{\sigma}$ is the spin of the scattering electron and $J_+$ and $J_-$ are the ladder operators within the $J$-multiplet ($\sigma_+$ and $\sigma_-$ are the analogous ladder operators for the spin )[3,9,10]. A spin-flip scattering event changes

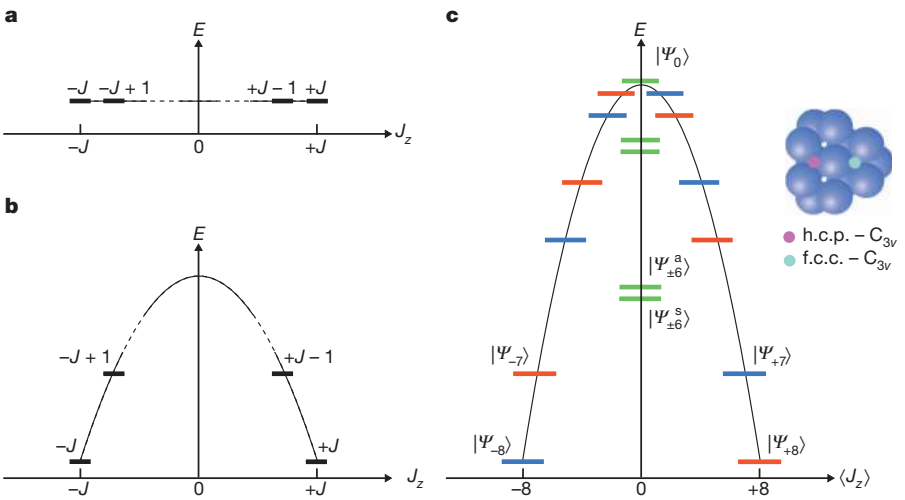


**Figure 1 | Magnetic sublevels of atoms with a total angular momentum J. a**, Degenerate sublevels of a free atom. **b**, Sublevels split by uniaxial anisotropy. **c**, The states mix in the presence of a crystal-field Hamiltonian of $C_{3v}$ symmetry. The degenerate green states split into symmetric (s) and antisymmetric (a) states. The inset shows the f.c.c. and h.c.p. adsorption sites.

[1]Physikalisches Institut, Karlsruhe Institute of Technology (KIT), Wolfgang-Gaede-Straße 1, 76131 Karlsruhe, Germany. [2]Institute of Solid State Physics, University of Tokyo, 5-1-5 Kashiwanoha, Kashiwashi, Chiba 277-8581, Japan. [3]Max-Planck-Institut für Festkörperforschung, Heisenbergstraße 1, 70569 Stuttgart, Germany. [4]Institut für Theoretische Festkörperphysik, Karlsruhe Institute of Technology (KIT), Wolfgang-Gaede-Straße 1, 76131 Karlsruhe, Germany. [5]Max-Planck-Institut für Mikrostrukturphysik, Weinberg 2, 06120 Halle, Germany. [6]Institut für Physik, Martin-Luther-Universität Halle-Wittenberg, 06099 Halle, Germany. [7]Wilhelm-Ostwald-Institut für Physikalische und Theoretische Chemie, Universität Leipzig, Linnéstraße 2, 04103 Leipzig, Germany.

$J_z$ by $\pm\hbar$. From this, one could conjecture that a complete reversal over the full barrier is strongly suppressed because it requires at least $2J$ scattering events and the energy barrier is large compared to thermal energies at cryogenic temperatures (for example, 0.34 meV at 4 K). This raised the hope of storing a magnetic bit in the two ground states.

However, in spite of the high magnetic anisotropy, the actual stability of the ground state is very limited owing to the strong hybridization of the 3*d* states of the transition atom with the substrate electrons. This leads to lifetimes of the excited states of the order of $\tau \approx 10$ fs (refs 4 and 6) and to an energy smearing of the excited states of the order of the barrier height due to the Heisenberg uncertainty principle. As a result, a reversal is possible without the need for thermal energy.

Longer lifetimes were achieved with atoms deposited on thin insulating films[5] where the interaction with the substrate electrons is weakened. In this case, a close inspection of the magnetic transitions induced by the tunnelling electrons of a scanning tunnelling microscope (STM) showed more transitions[3] than expected from the simple uniaxial Hamiltonian. In fact, the magnetic anisotropy of an adsorbed atom is hardly strictly uniaxial. Depending on the point symmetry of the adsorption site, additional terms enter the crystal-field Hamiltonian $\mathcal{H}$. In general, the crystal-field Hamiltonian can be written as:

$$\mathcal{H} = \sum_{n=0}^{\infty} \left( \sum_{m=0}^{n} B_n^m O_n^m + \sum_{m=1}^{n} \tilde{B}_n^m \tilde{O}_n^m \right), \qquad (2)$$

where $B_n^m$ and $\tilde{B}_n^m$ are the anisotropy constants and $O_n^m$ and $\tilde{O}_n^m$ are the crystal-field or Stevens operators. The latter are polynomials of order $n$ in the operators $J_z$, $J_+$ and $J_-$ with order $m$ in the ladder operators[11] and induce a zero-field splitting in the multiplet. Owing to time-reversal symmetry, states with opposite magnetic moment have the same energy for $\boldsymbol{B} = 0$. Thus, all terms with odd $n$ are forbidden. All terms with $m = 0$ only contain powers of $J_z$ and thus do not mix the $J_z$ eigenstates; for example, $O_2^0$ is essentially the already-introduced operator of the uniaxial anisotropy. All terms with $n > 2J$ vanish, because the operators act within the $2J + 1$ states of the multiplet. Likewise, terms with $n > 2l$ vanish, where $l$ is the orbital angular momentum of the individual electrons in the incomplete shell of the atom. Finally, all operators vanish that are incompatible with the point symmetry of the adsorption site; for example, all $\tilde{B}_n^m$ vanish for a mirror plane normal to the surface.

In the following, we concentrate on atoms adsorbed in three-fold hollow sites of the (111) surface of face-centred cubic (f.c.c.) crystals. Both the f.c.c. and the hexagonal close-packed (h.c.p.) adsorption sites have a three-fold symmetry with a vertical mirror plane (and its rotations) perpendicular to the surface (see inset of Fig. 1c), that is, a $C_{3v}$ symmetry. Encouraged by a previous study[12], we used rare earth atoms instead of transition metals, because the magnetic anisotropies of the former are typically larger than those of 3*d* atoms, and their 4*f* orbitals hybridize less with the substrate, resulting in potentially longer lifetimes. Thus, for rare earth atoms (with $l = 3$) in zero magnetic field the Hamiltonian can be written as[13]:

$$\mathcal{H} = B_2^0 O_2^0 + B_4^0 O_4^0 + B_6^0 O_6^0 + B_4^3 O_4^3 + B_6^3 O_6^3 + B_6^6 O_6^6. \qquad (3)$$

The operators $O_n^m$ are given explicitly in the Supplementary Information. Although the first three terms do not mix the $J_z$ eigenstates, the last three mix $J_z$ states differing in $J_z$ by 3 or 6.

The energy spectrum of the Hamiltonian (equation (3)) for a holmium (Ho) impurity ($J = 8$, with ten 4*f* electrons[14]) and dominating, negative $B_2^0$ is illustrated in Fig. 1c. Overall, the parabolic energy dependence is preserved when the states are plotted according to their expectation value of $J_z$. Every eigenstate is a mixture of several $|J_z\rangle$ states differing by $\Delta J_z = \pm 3$ and thus three classes of eigenstates form, marked in Fig. 1c by three different colours. Of the states marked in green, the $|\pm 3\rangle$ and $|\pm 6\rangle$ states are pairwise degenerate when considering only the first three operators in equation (3). They are, however, strongly mixed by the last three operators, resulting in new non-magnetic, energy-split states of different symmetry ('s' for symmetric and 'a' for antisymmetric). The red and the blue states form degenerate doublets.

In general, depending on $J$, three cases can arise. First, the two ground states may be of the same colour and get strongly mixed and split. This scenario is often called the tunnelling case. The eigenstates are not pure in $J_z$, so the preparation of a pure state leads to tunnelling to a state of reversed magnetization by the Stevens operators alone, and consequently to short relaxation times[5]. Second, the two ground states $\Psi_{-J}$ and $\Psi_{+J}$ do not mix, but are linked by spin-flip transitions due to $\mathcal{V}$ (see equation (1)). This is the so-called Kondo case where scattering with a single electron can lead to transitions between the two ground states with zero energy cost. Again, lifetimes are short. At low temperatures the conduction electrons can even form a Kondo singlet with the atom. Third, the transition between the two ground states by scattering with a single electron is forbidden (that is, the matrix element of $\mathcal{V}$ vanishes). Thus, the magnetic moment of the atom is decoupled from the electrons of the substrate to first order, and reversal is possible only by sequential scattering via intermediate states of higher energy. Depending on the excitation energy, these processes can be suppressed at low temperatures, effectively restoring the barrier and leading to long lifetimes.

The last scenario is realized for Ho on Pt(111), that is, $\langle \Psi_{-8} | \mathcal{V} | \Psi_{+8} \rangle = 0$. This is a consequence of the combination of the symmetries and the value of $J$ and follows from group-theoretical arguments. To show this, we investigate how the matrix element $\langle \Psi_{-8} | J_i | \Psi_{+8} \rangle$, where $i \in \{x, y, z\}$, behaves under time reversal. For $\boldsymbol{B} = 0$, $\mathcal{H}$ commutes with the time-reversal operator $\mathcal{T}$, and $\mathcal{T} J_i = -J_i \mathcal{T}$. Further, $\mathcal{T}^2 = 1$ because the number of electrons in Ho is even, $\mathcal{T} |\Psi_{\pm 8}\rangle = |\Psi_{\mp 8}\rangle$ (see Supplementary Information) and $\mathcal{T}$ is anti-unitary, that is, $\langle \chi | \phi \rangle = \langle \mathcal{T}\phi | \mathcal{T}\chi \rangle = \langle \mathcal{T}\chi | \mathcal{T}\phi \rangle^*$, where the asterisk indicates the complex conjugate. Thus we can write:

$$\begin{aligned} \langle \Psi_{-8} | \overbrace{J_i | \Psi_{+8} \rangle}^{|\phi\rangle} &= \langle \mathcal{T}\Psi_{-8} | \mathcal{T} J_i \Psi_{+8} \rangle^* \\ &= -\langle \Psi_{+8} | J_i \mathcal{T} \Psi_{+8} \rangle^* = -\langle \Psi_{+8} | J_i | \Psi_{-8} \rangle^* \\ &= -\langle \Psi_{-8} | J_i | \Psi_{+8} \rangle, \ i \in \{x, y, z\} \end{aligned} \qquad (4)$$

Thus, the matrix elements of $\boldsymbol{J}$ vanish as a consequence of symmetries and direct transitions between the ground states cannot be induced by scattering electrons. We expect long lifetimes at low temperatures.

In the experiments, Ho atoms were deposited on a clean Pt(111) substrate at 4.4 K, leading to individual Ho atoms on the surface (adatoms) as seen by low-temperature STM (compare Fig. 2a). First, a non-magnetic tungsten tip was used to image the surface and investigate excitations of the atom. The second derivative of the tunnelling current $I$ was measured as function of the bias voltage $V$, while positioning the tip over the Ho atoms, as shown in Fig. 2b. The $d^2I/dV^2$ spectra taken at 4.4 K reveal the typical dip–peak structure at a bias voltage $V_{sf}$, as seen in many other single-atom systems[4,6,12]. Peak and dip are well separated, speaking for an inelastic excitation as opposed to the Kondo effect. As shown later by spin-polarized STM measurements, this excitation is magnetic and corresponds to a spin-flip transition from the ground state to the first excited state. The analysis of the spectra of many atoms reveals that the excitation energy of atoms in f.c.c. sites (about 8 meV) is higher than in h.c.p. sites (about 6 meV) and that the adsorption energy of f.c.c. sites is higher (see Supplementary Information).

The anisotropy constants can also be obtained from first principles, by applying a first-order perturbation theory[15] (see the Supplementary Information for more details). These calculations confirm that Ho on Pt(111) is indeed in a $J = 8$ state and shows an out-of plane easy axis. For f.c.c. Ho atoms, the first excited magnetic state is 7.7 meV above the ground state, in good agreement with the experimental observation.

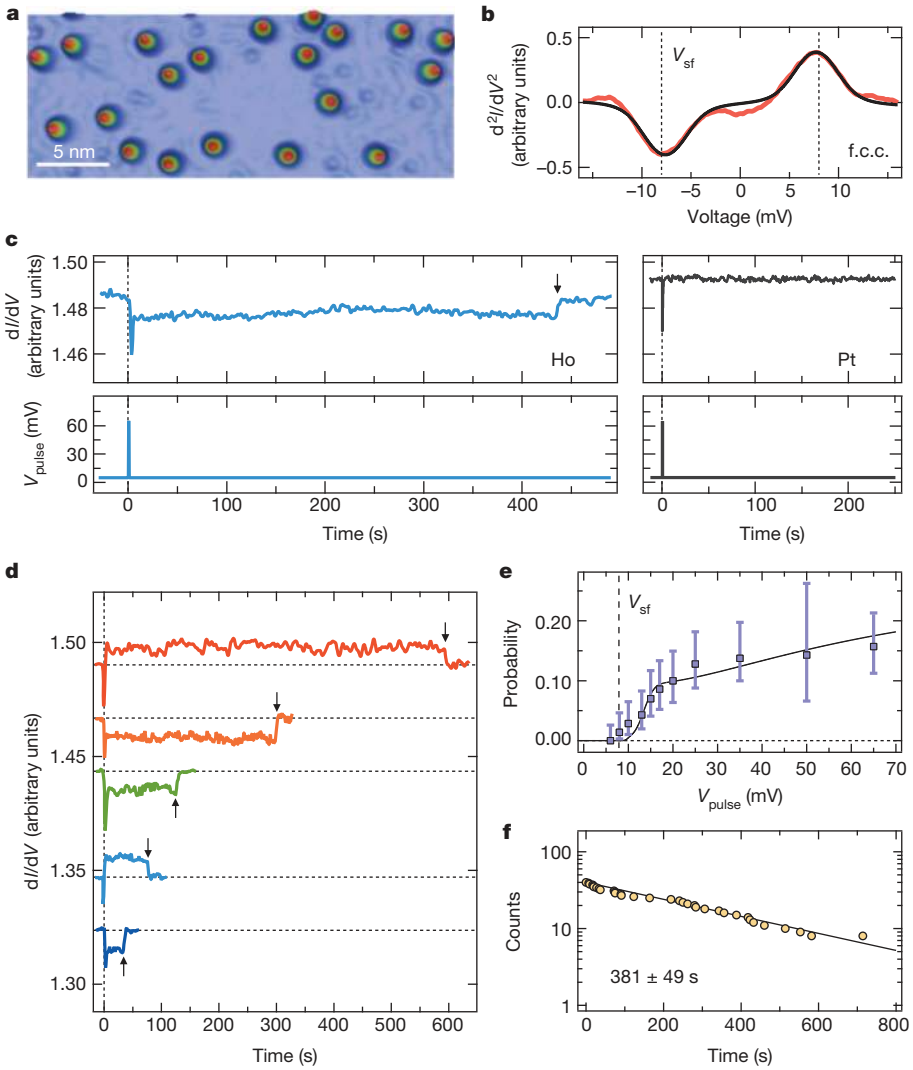


**Figure 2 | Magnetic behaviour of Ho atoms ($J = 8$) adsorbed on Pt(111).** **a**, Three-dimensional topographic STM image of single Ho atoms adsorbed on Pt(111) at 4.4 K. **b**, Inelastic tunnelling spectrum ($d^2I/dV^2$) recorded on top of a single Ho atom in the f.c.c. position (red), showing an inelastic excitation at $V_{sf} \approx 8$ meV, as determined by a fit to the data (black). **c**, Time traces of the $dI/dV$ signal recorded with a spin-polarized tip on a Ho atom in the f.c.c. position and on bare Pt ($V = 5$ mV, $I = 1$ nA). At $t = 0$ a voltage pulse $V_{pulse}$ above the inelastic excitation threshold was applied. Although on bare Pt(111) no changes of the $dI/dV$ signal were observed, the pulse induced a magnetic transition between the two ground states of Ho, as deduced from the observed change of the spin-polarized $dI/dV$ signal. After some delay, the atoms spontaneously switch back to the initial state, as seen by a second change of the signal (indicated by arrow). **d**, A series of switching measurements of Ho atoms representing a wide range of the decay times indicated by arrows. **e**, Magnetic switching probabilities and their standard deviation as function of the pulse height as well as a fit (black line) to the data obtained from a master equation for the induced transitions. **f**, Decay of 40 states prepared by pulses (dots) and an exponential fit (black line).

In the following we address atoms on the high-anisotropy f.c.c. site only. The large magnetic excitation energy would lead to a stable magnetic moment at low temperatures, because we expect from theory that scattering with the electron bath cannot directly switch the magnetization of the atom between the two ground states. Only if a scattering electron (from the tunnelling current, for example) has sufficient energy can it bring the atom from the ground state to the first excited state, which in turn can relax to either of the two ground states via a second inelastic scattering event with substrate electrons.

To investigate this scenario, we carried out spin-polarized STM measurements with anti-ferromagnetic tips that have a spin polarization perpendicular to the surface[16]. We stabilized the tip over a Ho atom at $I = 1$ nA and $V = 5$ mV, which is below the excitation threshold. Thus, the tunnelling electrons cannot switch the atom but probe the spin polarization on top of the atom. The $dI/dV$ signal depends on the relative orientation of the tip magnetic moment and the Ho moment. Then we applied 0.2-ms voltage pulses, while the feedback was turned off. If the atom switches between the two ground states during the pulse, the $dI/dV$ signal is different before and after the pulse. We varied the height of the pulse up to 65 mV.

Figure 2c shows examples of recorded time traces of the $dI/dV$ signal at 1.1 K in cases where we observed a switching and, for comparison, on bare Pt(111). The spin signal recorded above the atom has two distinct values representing the two magnetic ground states with the magnetization perpendicular to the surface, whereas the signal on Pt(111) is not influenced by the pulse, thus excluding tip changes. After switching the magnetic moment of the Ho atom, it stays in the reversed state for times in the range from seconds to minutes until it spontaneously switches back, as indicated by the arrows in Fig. 2d. This illustrates long lifetimes, as will be discussed below.

By applying many pulses to an individual atom, we determined the probability that a voltage pulse leads to a reversal of the magnetic state (see Fig. 2e). In agreement with the inelastic spectrum, we observe a threshold for reversal at about 8 mV. Above this, the switching probability per pulse increases continuously owing to the increase of the tunnelling current with pulse voltage, because the feedback loop is opened during the pulse. The switching probability depends on the branching ratio of the relaxation from the excited states to either of the ground states, so the switching probability contains information about the anisotropy constants. The solid line in Fig. 2e was calculated using a master equation of the dynamics of the states' population with anisotropy constants determined from first principles and fitting the coupling strength of the Ho spin to the substrate and tunnelling electrons (for details see the Supplementary Information). The switching probabilities for higher-voltage pulses depend strongly on the tip spin polarization, which can be determined from the fit to be about 20%. The curve fits the experimental data excellently, confirming the quantum mechanical nature of the Ho spin.

To investigate the stability of the ground states, we repeated the switching experiment 40 times and plotted the observed population

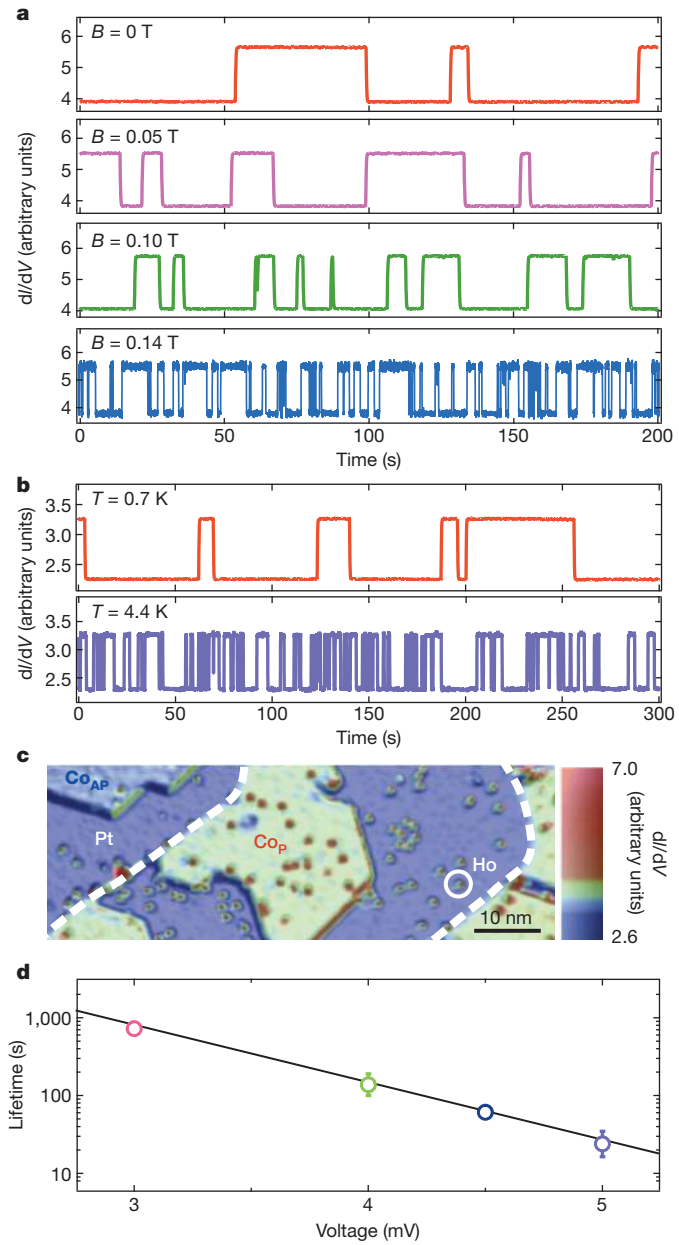


**Figure 3 | Lifetimes of adsorbed Ho atoms as function of external parameters.** **a**, Spontaneous transitions between the two ground states for different magnetic fields along the surface normal observed with spin-polarized d$I$/d$V$ signal recorded at 0.7 K, 5 mV and 50 nA. **b**, Spontaneous transitions between the two ground states for two different temperatures without applied magnetic field recorded at 5 mV and 50 nA. **c**, Spin-polarized d$I$/d$V$ map of Ho atoms and Co islands on Pt(111) ($V = 300$ mV, $I = 1.5$ nA). Two distinct signals are observed on Co islands magnetized parallel (P) and antiparallel (AP) to the tip. Positions of Pt atomic steps are indicated by dashed lines. **d**, Lifetimes extracted from spontaneous transitions at 0.7 K without applied magnetic field and 1 nA as function of sample bias on the marked Ho atom in **c**. Error bars represent the standard deviation of a fit to an exponential decay (28, 23, 102 and 94 transitions for 3.0-mV, 4.0-mV, 4.5-mV and 5.0-mV sample biases, respectively).

decay (see Fig. 2f). The data follow a simple exponential decay with a lifetime $\tau$ of 381 ± 49 s, indicating an efficient decoupling of the Ho spin from the conduction electrons.

To understand the value of $\tau$, we turn back to the original explanation: direct transitions between the ground states by tunnelling and single spin-flip events are forbidden due to the time-reversal symmetry. Thus, transitions between the ground states can only be achieved by excitation to the first (or higher) excited state by substrate or tip electrons in the high energy tail of the thermal distribution or by breaking time-reversal symmetry using a magnetic field. To verify this, we investigated the dependence of $\tau$ on bias voltage, temperature and magnetic field.

Figure 3a illustrates the effect of a magnetic field applied perpendicularly to the surface at a temperature of 0.7 K. Similarly to the previous experiments, the spin-polarized d$I$/d$V$ signal on top of a Ho atom was recorded as a function of time. To increase the signal-to-noise ratio, a larger tunnelling current of 50 nA was used while keeping $V = 5$ mV. In this experiment, we did not apply pulses but observed spontaneous transitions between the two ground states. An increase of the switching frequency can be clearly observed with increasing magnetic field because spin-flip scattering between the two ground states is no longer forbidden (for details see the Supplementary Information). Similarly, $\tau$ decreases with increasing temperature, as illustrated in Fig. 3b ($V = 5$ mV, $I = 50$ nA).

To study the bias dependence, a different sample was used. Figure 3c shows a spin-polarized image (d$I$/d$V$ map) of adsorbed Ho atoms. To verify the spin-polarization of the tip, Co islands were deposited that decorate the step edges of the Pt(111) substrate. The Co islands are magnetized out-of-plane[17] and the contrast between the two islands indicates that the tip is sensitive to the out-of-plane magnetization. Figure 3d shows $\tau$ as a function of $V$ ($I = 1$ nA, $T = 0.7$ K), obtained by analysis of spontaneous transitions. Even though the bias voltages are below the first excitation energy, $\tau$ drops exponentially with rising voltage. This is due to the exponentially increasing number of thermal tunnelling electrons at higher bias voltages that have enough energy to excite the atom to the first excited state. Owing to the close proximity to the Co island, the Ho atom experiences a non-vanishing magnetic stray field of the island. This leads to a shorter $\tau$ at 5 mV than in the first measurement in spite of the lower temperature. However, at a 3 mV bias voltage, the lifetime is much longer, $\tau = 729 \pm 12$ s.

An interesting side effect of the forbidden spin-flip scattering by conduction electrons is that magnetic interactions between Ho atoms mediated by the Rudermann–Kittel–Kasuya–Yosida (RKKY) interaction[18] do not cause the exchange of angular momentum to lowest order, such that the observed $\tau$ is nearly independent of the local arrangement of the Ho atoms, as discussed in the Supplementary Information.

In conclusion, general symmetry requirements open up a new pathway to stabilize the magnetic moment of adsorbed atoms and decouple it from conduction electrons and nuclear spins. This method could potentially be used in data storage and quantum computing. By applying a magnetic field, the interactions could be switched back on, thus allowing controlled quantum manipulation of the spins.

## METHODS SUMMARY

The Pt(111) sample was cleaned by argon-ion sputtering followed by annealing to 850 K. The sample surfaces were checked for impurities by STM at 4.4 K before deposition of Ho. Ho atoms were deposited onto the clean surfaces at 4.4 K directly in the STM. Unpolarized STM tips were prepared from tungsten wires and were cleaned *in situ* by flashing to above 2,500 K. Spin-polarized tips were prepared by depositing about 20 monolayers of Mn or Cr *in situ* onto the tip apex followed by gentle annealing. Inelastic d$^2I$/d$V^2$ spectra were recorded using a modulation frequency of about 16 kHz at a root-mean-square voltage of 2.4 mV and detecting the second harmonics with a lock-in technique. Spin-polarized STM measurements were performed recording the d$I$/d$V$ signal with coated tips using a modulation of 720 Hz and 1 mV root-mean-square voltage. Voltage pulses were given with the feedback loop open to avoid destabilizing the tip position. Tip changes due to voltage pulses were excluded by checking between every measurement on Ho atoms also the time trace of pulses given on bare Pt(111). For tests of the out-of-plane sensitivity of the spin-polarized tips, one monolayer high Co islands were grown on Pt(111) at 360 K before inserting the sample into the STM. All experiments were performed using a home-built cryogenic Joule–Thomson cooled STM[19].

First-principles calculations were carried out within the density functional theory. The crystalline structure was determined with the Vienna Ab-initio Simulation Package (VASP) method, well known for providing precise total energy and

forces[20,21]. The obtained structural information was further used for calculations of the electronic and magnetic properties of single Ho atoms on the Pt(111) surface using a self-consistent relativistic full-charge Green's function method, which is specially designed for semi-infinite systems and embedded real-space clusters[22,23]. A self-interaction correction method and a local density approximation (LDA) approximation including Hubbard $U$ corrections were applied to provide an adequate description of strongly localized Ho $f$ electrons[24,25].

**Received 15 August; accepted 9 October 2013.**


1. Gambardella, P. *et al.* Giant magnetic anisotropy of single cobalt atoms and nanoparticles. *Science* **300,** 1130–1133 (2003).
2. Heinrich, A. J., Gupta, J. A., Lutz, C. P. & Eigler, D. M. Single-atom spin-flip spectroscopy. *Science* **306,** 466–469 (2004).
3. Hirjibehedin, C. F. *et al.* Large magnetic anisotropy of a single atomic spin embedded in a surface molecular network. *Science* **317,** 1199–1203 (2007).
4. Balashov, T. *et al.* Magnetic anisotropy and magnetization dynamics of individual atoms and clusters of Fe and Co on Pt(111). *Phys. Rev. Lett.* **102,** 257203 (2009).
5. Loth, S., Etzkorn, M., Lutz, C. P., Eigler, D. M. & Heinrich, A. J. Measurement of fast electron spin relaxation times with atomic resolution. *Science* **329,** 1628–1630 (2010).
6. Khajetoorians, A. A. *et al.* Itinerant nature of atom-magnetization excitation by tunneling electrons. *Phys. Rev. Lett.* **106,** 037205 (2011).
7. Loth, S., Baumann, S., Lutz, C. P., Eigler, D. M. & Heinrich, A. J. Bistability in atomic-scale antiferromagnets. *Science* **335,** 196–199 (2012).
8. Khajetoorians, A. A. *et al.* Current-driven spin dynamics of artificially constructed quantum magnets. *Science* **339,** 55–59 (2013).
9. Fransson, J. Spin inelastic electron tunneling spectroscopy on local spin adsorbed on surface. *Nano Lett.* **9,** 2414–2417 (2009).
10. Schuh, T. *et al.* Magnetic anisotropy and magnetic excitations in supported atoms. *Phys. Rev. B* **84,** 104401 (2011).
11. Bleaney, B. & Stevens, K. W. H. Paramagnetic resonance. *Rep. Prog. Phys.* **16,** 108–159 (1953).
12. Schuh, T. *et al.* Magnetic excitations of rare earth atoms and clusters on metallic surfaces. *Nano Lett.* **12,** 4805–4809 (2012).
13. Wybourne, B. G. *Spectroscopic Properties of Rare Earths* Ch. 4.4, 166 (Wiley, 1965).
14. Coey, J. M. D. *Magnetism and Magnetic Materials* 114 (Cambridge Univ. Press, 2009).
15. Richter, M., Oppeneer, P., Eschrig, H. & &Johansson, B. Calculated crystal-field parameters of $SmCo_5$. *Phys. Rev. B* **46,** 13919–13927 (1992).
16. Wiesendanger, R. Spin mapping at the nanoscale and atomic scale. *Rev. Mod. Phys.* **81,** 1495–1550 (2009).
17. Rusponi, S. *et al.* The remarkable difference between surface and step atoms in the magnetic anisotropy of two-dimensional nanostructures. *Nature Mater.* **2,** 546–551 (2003).
18. Zhou, L. *et al.* Strength and directionality of surface Ruderman-Kittel-Kasuya-Yosida interaction mapped on the atomic scale. *Nature Phys.* **6,** 187–191 (2010).
19. Zhang, L., Miyamachi, T., Tomanić, T., Dehm, R. & Wulfhekel, W. A compact sub-Kelvin ultrahigh vacuum scanning tunneling microscope with high energy resolution and high stability. *Rev. Sci. Instrum.* **82,** 103702 (2011).
20. Kresse, G. & Furthmüller, J. Efficient iterative schemes for ab initio total-energy calculations using a plane-wave basis set. *Phys. Rev. B* **54,** 11169–11186 (1996).
21. Hafner, J. Ab-initio simulations of materials using VASP: density-functional theory and beyond. *J. Comput. Chem.* **29,** 2044–2078 (2008).
22. Lüders, M., Ernst, A., Temmerman, W. M., Szotek, Z. & Durham, P. J. Ab initio angle-resolved photoemission in multiple-scattering formulation. *J. Phys. Condens. Matter* **13,** 8587–8606 (2001).
23. Zeller, R. & Dederichs, P. H. Electronic structure of impurities in Cu, calculated self-consistently by Korringa-Kohn-Rostoker Green's-function method. *Phys. Rev. Lett.* **42,** 1713–1716 (1979).
24. Perdew, J. P. & Zunger, A. Self-interaction correction to density-functional approximations for many-electron systems. *Phys. Rev. B* **23,** 5048–5079 (1981).
25. Anisimov, V. I., Zaanen, J. & Andersen, O. K. Band theory and Mott insulators: Hubbard $U$ instead of Stoner $I$. *Phys. Rev. B* **44,** 943–954 (1991).


**Supplementary Information** is available in the online version of the paper.

**Acknowledgements** We acknowledge funding by the German Science Foundation (DFG) grant number Wu 349/4-2, the DFG priority programme SPP 1538 Spin Caloric Transport and the DFG Collaborative Research Centre SFB 762 Functionality of Oxide Interfaces. The calculations were performed at the Rechenzentrum Garching of the Max Planck Society.

**Author Contributions** W.W. conceived the experiments, and T. Miyamachi, T.S., T. Märkl, A.S. and C.B. carried them out. The data were analysed by T. Miyamachi, T.S., T. Märkl, C.B., T.B. and W.W. Group theory of the crystal field was performed by T.S., T.B., C.B. and W.W. Master equations were analysed by C.K., S.A., M.M. and G.S. Ab initio calculations were performed by M.H., M.G., S.O., W.H., I.M. and A.E. The manuscript was written by T.B. and W.W. Figures were prepared by T. Miyamachi. All authors discussed the results and commented on the manuscript.

**Author Information** Reprints and permissions information is available at www.nature.com/reprints. The authors declare no competing financial interests. Readers are welcome to comment on the online version of the paper. Correspondence and requests for materials should be addressed to W.W. (wulf.wulfhekel@kit.edu).